ACS OMEGA

http://pubs.acs.org/journal/acsodf

Article

Water-Soluble Poly(vinyl alcohol)/Biomass Waste Composites: A New Route toward Ecofriendly Materials

Guoliang Tian, Li Li, Yijun Li,* and Qi Wang

Cite This: *ACS Omega* 2022, 7, 42515−42523

Read Online

ACCESS | Metrics & More | Article Recommendations | Supporting Information

ABSTRACT: With the intention to abate the pollution arising from the improper handling of petroleum-based plastic, green composites consisting of biodegradable plastics and biomass wastes have received widespread attention. However, the balance between mechanical performance and biodegradability still has not been reconciled and evaluated. Herein, a concept for water-soluble poly(vinyl alcohol) (PVA)/biomass waste composite materials is proposed. Instead of degrading to small molecules, the PVA matrix can dissolve in water within the soil. Moreover, after PVA was composited with waste cottonseed shell (CTS) using solid-state shearing milling (S^3M) technology, considerable mechanical and thermal performance was achieved, with the maximum tensile strength and degradation temperature of the PVA/CTS composites reaching 10.3 MPa and ∼250 °C, respectively. Moreover, the soil burial test demonstrated that even if PVA cannot degraded in environment within a short term, its water-soluble nature ensures its environmental friendliness, as the PVA matrix can dissolve in soil in 10 days without imposing any adverse effects on either plants (wheat) or animals (earthworm). This work not only describes the preparation a series of ecofriendly PVA/biomass composites but also provides new insight into the environmental friendliness of PVA-based materials.

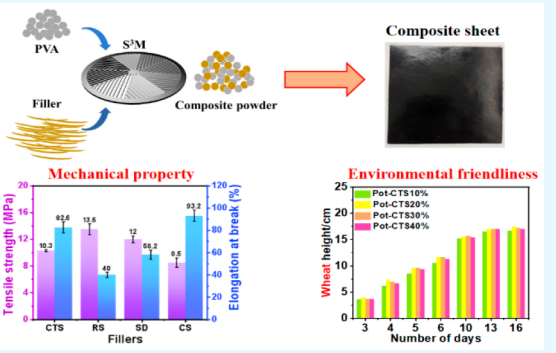

INTRODUCTION

Plastics have been widely used as packaging material due to their industrial applicability and advantageous properties, including robust mechanical properties, versatility, low cost, and gas-barrier property.[1−3] However, owing to improper disposal and management, a tremendous amount of plastic waste has been deposited in the environment.[1,4,5] The high stability of plastics is a double-edged sword, making it difficult for them to degrade in the environment and allowing them to persist in natural soil for centuries.[6,7] The wasted packaging material is also a source of microplastics, which severely threaten both the environment and human health.[8] Therefore, it is of great urgency to develop environmentally friendly polymer materials.

Biodegradable plastics are a new generation of polymers that are manufactured as promising substitutes for nondegradable plastics to resolve plastic pollution.[3,9] The biodegradable plastics, such as polycaprolactone,[10,11] poly(lactic acid),[12−14] polyhydroxyalkanoates (PHAs),[9] and poly(butylene succinate),[15−17] can degrade into smaller molecules via the effect of microorganisms in a suitable environment.[18,19] Nevertheless, the nature of the disposal environment plays a significant role, as it directly determines the number and activity of microorganisms in the process of biodegradation.[20] Consequently, it is still difficult to achieve complete degradation in natural conditions, as the plastics tend to be fragmented into minute pieces and become another potential threat to the ecological safety of soil ecosystems.[20,21] Furthermore, the high cost of biodegradable plastics also restricts their extensive application.[15,22] Therefore, the green alternative of water-soluble and easily recycled polymeric materials has been gradually followed with intensive interest.[23]

Poly(vinyl alcohol) (PVA) featuring abundant hydroxyl groups is a typical water-soluble polymer and has been extensively employed in food and pharmaceutical packaging.[24−27] Although PVA is also regarded as a biodegradable and biocompatible polymer, severe degradation conditions such as specific strain, temperature, and humidity make it a challenge to achieve the sole utilization of PVA.[20] Agricultural residues, such as cottonseed shell, reed straw, sawdust, corn stalk, bamboo, and bagasse, are produced in large quantities annually. They consist of cellulose, hemicellulose, and lignin and thus have been identified as the most abundant renewable resources.[28−30] Incorporating PVA with biomass materials is a good solution to prepare biocomposites with better mechanical performance and biodegradability, since the many hydroxyl groups in PVA are keen to form hydrogen bonds with those in

Received: September 7, 2022
Accepted: October 28, 2022
Published: November 9, 2022

https://doi.org/10.1021/acsomega.2c05810
ACS Omega 2022, 7, 42515−42523

the cellulose and hemicellulose, which guarantees the compatibility of PVA and agricultural residues.[31,32] For instance, Haque[33] prepared PVA/cotton gin trash (CGT) biocomposite films by the solution-casting method and demonstrated that CGT enhanced the tensile strength and thermal stability. Balavairavan[34] fabricated a series of biodegradable PVA composite films with green banana peel filler (GBPF) and confirmed that the PVA/GBPF biofilms presented better biodegradation properties. However, these works ignore the impact of the water solubility of PVA on the environment.[35]

In this study, PVA/cottonseed shell (CTS) composites were first preprocessed into a composite powder via solid-state shear milling (S^3M) technology, where a well-dispersed morphology and interface compatibility were achieved via the mechano-chemical effects of S^3M.[36] Subsequently, the composite powder was compression molded to clarify the structure−performance relationship as well as the potential impact on soil. There are three issues addressed: (i) the relationship between the morphology and the structure of the PVA/biomass composites, (ii) the contribution of water solubility and biodegradability in PVA, and (iii) the universality of this method. This work not only describes the preparation of a series of PVA/biomass waste composites but also provides new insight for understanding the environmental friendliness of PVA-based materials.

EXPERIMENTAL SECTION

Materials. PVA powder of 100 mesh, with a degree of polymerization of 1750 ± 50 and a degree of hydrolysis of 88%, was purchased from SINOPEC Sichuan Vinylon Works, China. The CTS powder of 100 mesh was obtained from farmland in Shandong. Additional biomass waste such as reed straw (RS), sawdust (SD), and cornstalk (CS) were purchased from Changyuan Straw Processing Factory, Shangxi Wood Products Firm, and Surui Straw Processing Factory, respectively, in Jiangsu, China.

Preparation of the PVA/CTS Powder. PVA and CTS powder with a mass ratio of 6:4 was first mixed by a high-speed mixer (RS-FS1406, Royalstar, China) to prepare a master batch. After the CTS content was diluted to 10, 20, 30, and 40 wt % of the total amount of mixture by the addition of pure PVA, various PVA/CTS mixtures were dried in an oven at 80 °C for 24 h and then treated by S^3M equipment for 10 cycles at room temperature. The speed of the equipment was set at 30 rpm, and the pressure was controlled at 5 MPa. Details of the S^3M technique have been reported in the relevant literature.[37] The as-prepared composite powder was designated as PVA-CTS-X, where X represented the mass fraction.

Preparation of the PVA/CTS Composites. A deionized water/glycerin solution with mass ratio of 1:2 was added to the PVA/CTS powder as plasticizer by a high-speed mixer at room temperature, and the samples were kept in an oven at 40 °C for 48 h to make the plasticizer penetrate. The weight ratio of the plasticizer and the powder was kept at 3:7. The composite sheets were compression molded into square specimens with a length of 100 mm and a thickness of 1 mm. During processing, all samples were first pressed at 170 °C under a pressure of 10 MPa for 5 min, then heating was discontinued without changing the pressure until the temperature returned to room temperature.

CHARACTERIZATION

Evaluation of the Water Solubility of PVA. The water solubility of all samples was measured as follows: 1 g PVA sheets were set in beaker with 50 mL of deionized water at the expected temperature. After the removal of the undissolved part, PVA was dried in oven at 80 °C for 12 h. Then, the mass loss percentage ($D(\%)$) could be calculated using the following equation:

$$D(\%) = \frac{m_1}{m_0} \times 100\% \quad (1)$$

where m_1 is the mass of the undissolved part of the sample and m_0 is the total mass of the sample used for the water-solubility measurement, which was 1 g in this case.

Morphological Evolution of the Biomass Waste during S^3M. The particle distribution of the composite particle was assessed by laser light diffraction using a particle size analyzer (S3500-SI, Microtrac Instrument Co., Ltd., USA). A small amount of composite particles was dispersed in absolute ethanol, and the particle size was measured after ultrasonic dispersion. The morphology of the as-prepared samples was investigated by an Inspect F field-emission scanning electron microscope (SEM, FEI Co., Ltd., USA) with an acceleration voltage of 10 kV. All samples were cryofractured in liquid nitrogen and sputtered with gold under a vacuum before testing.

Crystalline and Molecular Structures of the PVA/Biomass Waste Composites. Fourier transform infrared spectroscopy (FTIR) spectra of the composites were recorded by a Nicolet 6700 FT-IR spectrometer (Thermo Scientific, USA) in the attenuated total reflectance (ATR) mode with 32 scans from 4000 to 650 cm^{-1} at a 4 cm^{-1} scan resolution at room temperature. Spectra were baseline -corrected and analyzed using OMNIC ver. 8.1 software. X-ray diffraction (XRD) was employed to characterize the crystalline structures of the composites using a DX-1000 diffractometer (DanDong FangYuan Instrument Co., Ltd., China). The composite sheets were continuously scanned from 5° to 80° at a rate of 5°/s. The acceleration voltage was 40 kV ,and the electric current was 25 mA. Differential scanning calorimetry (DSC) curves were recorded on a Q20 system (TA Instruments, USA) with a heating rate of 10 °C/min from 40 to 250 °C under a continuous nitrogen atmosphere. The crystallinity of PVA and the composite sheets was calculated using the following equation:

$$X(\%) = \frac{\Delta H_f}{\Delta H_f^0} \times 100\%/C \quad (2)$$

where ΔH_f is the melting enthalpy of the sheets, ΔH_f^0 is the melting enthalpy of the 100% crystalline PVA 1788 (168 J/g),[38] and C is the mass fraction of PVA.

Mechanical Performance and Thermal Stability. The stress−strain curves of the samples were obtained by a universal tensile testing machine (RGL-10, Rieger Instrument Co., Ltd.) according to Chinese standard GB/T 1040-2006. All samples were evaluated at room temperature with a speed of 50 mm/min, and five specimens of each sample were tested to obtain the average and standard deviation values. Thermogravimetric analysis (TGA) was conducted on a TA Q50 thermogravimetric analyzer (TA Instrument, Co., USA) under a nitrogen atmosphere at a heating rate of 10 °C/min from 40 to 700 °C with a flow rate of 50 mL/min. Graphs of the weight loss versus temperature and the first derivative of the weight loss with respect to temperature (dW/dT) versus temperature were generated by Universal Analysis software.

Environmental Safety of the PVA/Biomass Waste Composites. The soil burial test was carried out on a laboratory scale. Composite sheets were cut into a rectangular

https://doi.org/10.1021/acsomega.2c05810
ACS Omega 2022, 7, 42515−42523

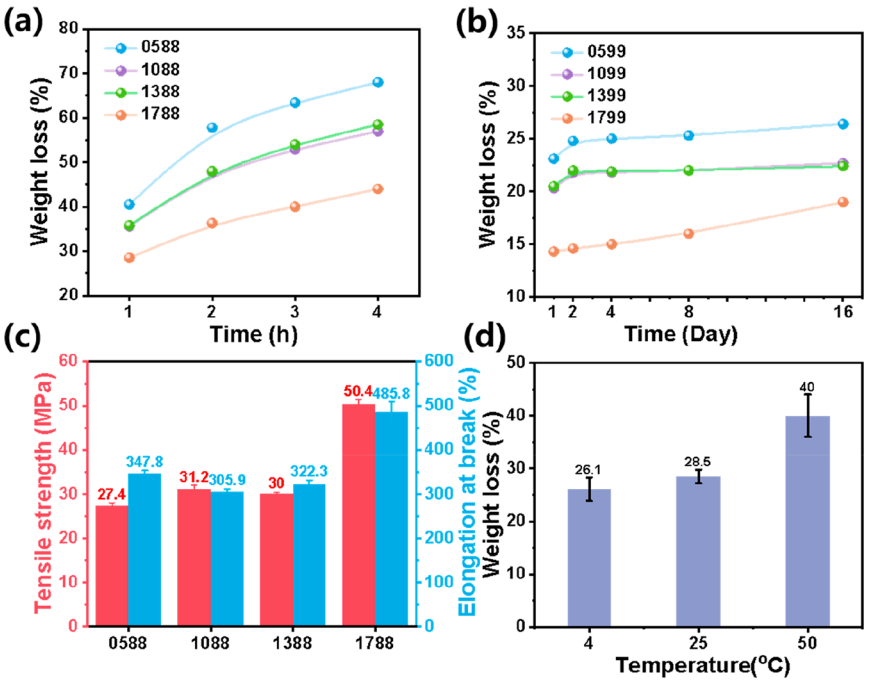

Figure 1. Plots of the weight loss of PVA with different molecular weights versus the soaking time with alcoholysis degrees of (a) 88% and (b) 99%. (c) Mechanical performance of different PVA matrices. (d) Weight loss of PVA 1788 in 1 h as a function of the water temperature.

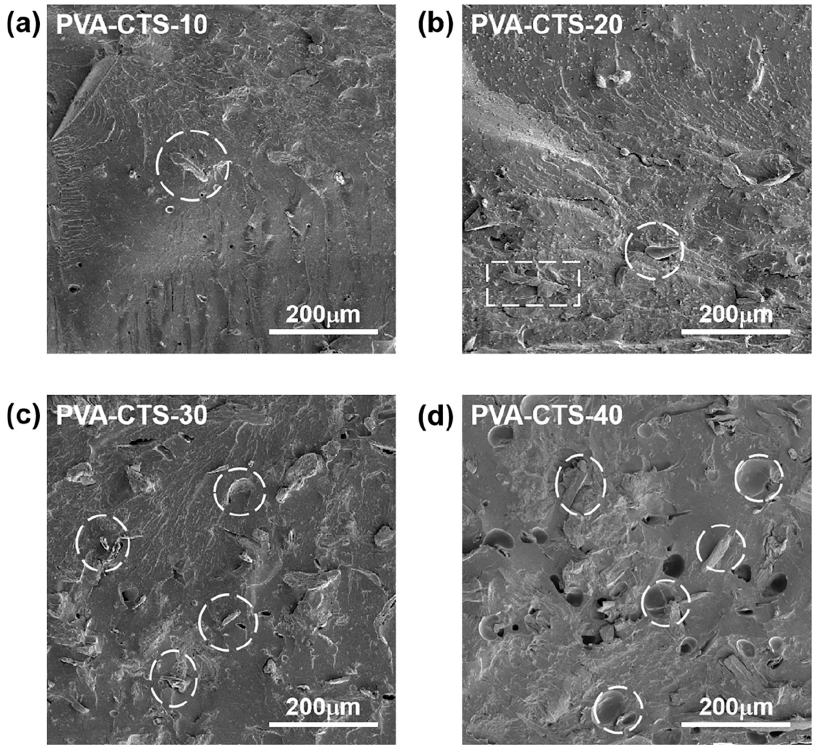

Figure 2. SEM images of the PVA/CTS composite sheets with (a) 10, (b) 20, (c) 30, and (d) 40 wt % loading.

shape (25 mm × 25 mm) and then buried in soil at a depth of 10 cm in an open container. Eighteen wheat seeds were planted in each pot, and the average height of the wheats was recorded regularly. Forty earthworms were shifted to pots containing PVA/CTS samples for two weeks, and the number of surviving earthworms was recorded in another test. The pots without composites were set as controls. During the experiment period, the pots were watered every 10 days to make up for water evaporation. Additionally, to study the effect of PVA on earthworms, another test was conducted. Twenty earthworms were kept in soil containing the PVA solution with a mass concentration of 0, 1, 3, 6g, or 9 g/kg. Aside from PVA, 20 g of amylaceum was add into soil samples to offer nutritious alternatives. The number of surviving earthworms was recorded after two weeks.

https://doi.org/10.1021/acsomega.2c05810
ACS Omega 2022, 7, 42515−42523

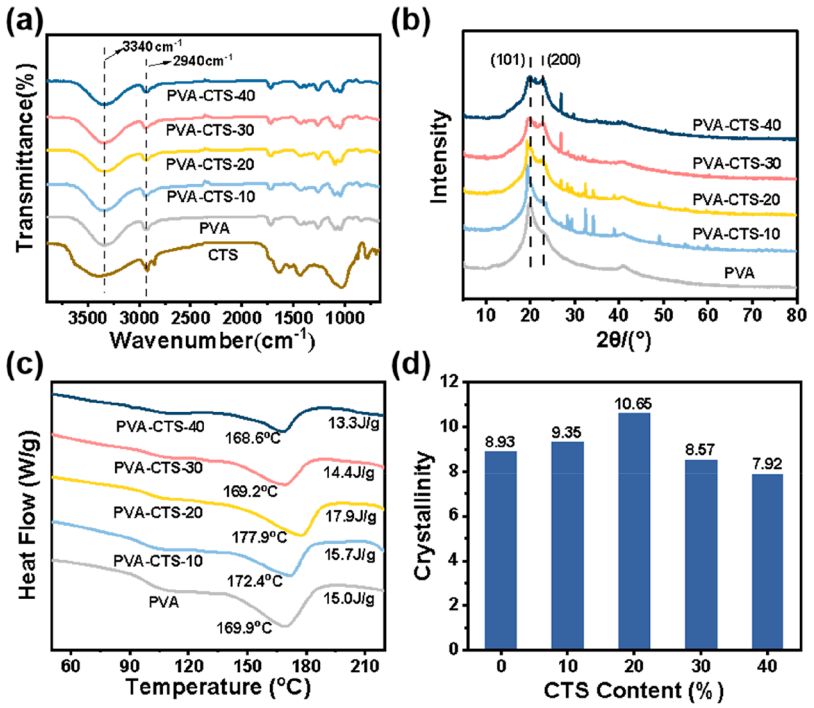

Figure 3. (a) FTIR curves, (b) XRD patterns, (c) DSC curves, and (d) crystallinity index histogram of PVA-CTS-(0−40) composite sheets.

RESULT AND DISCUSSION

Water Solubility and Mechanical Performance of the PVA Matrix. The concept of this study is based on the water solubility of PVA, which enables PVA to dissolve in soil and act as a moisturizer. Accordingly, the water solubility of commercially available PVA matrices with different grades was analyzed as a function of alcoholysis and molecular weight. For instance, 0588 referrs to PVA with the degree of polymerization of 500 and a degree of alcoholysis of 88%. As shown in Figure 1a and b, PVA with a lower molecular weight and an 88% alcoholysis degree exhibited considerable mass loss, while that with a 99% alcoholysis degree took four days. As demonstrated by Fuji,[39] the crystallinity and interchain hydrogen bonding exhibited a determining effect on the water solubility of PVA. The stronger intermolecular interaction in PVA with a 99% degree of alcoholysis, high crystallinity, and a high molecule weight consequently led to poor water solubility. Nevertheless, solubility enhancement will be accompanied by a weakening of the mechanical properties of PVA, so a suitable balance is needed to take into account practical applications and environmental friendliness. Figure 1c shows that PVA 1788 exhibited the highest tensile strength and elongation at break, while Figure 1d also demonstrates the adaptability of PVA 1788 at various ambient temperatures. Consequently, PVA 1788 was selected as the optimal candidate for the following test due to its good mechanical performance and moderate solubility.

Morphological and Crystalline Performance of PVA/CTS Composites. As a multihydroxyl polymer with strong intra- and intermolecular hydrogen bonds, PVA demonstrates excellent potential in terms of compounding with natural biomass materials, which consists of mainly cellulose and hemicellulose.[29] Nevertheless, cellulose is strongly adhered to hemicellulose and lignin through hydrogen bonds, forming a complex protective network and preventing the exposure of the active hydroxyl groups. Therefore, direct blending of PVA and biomass materials is often difficult, making it difficult to fully demonstrate its advantages and deteriorate the mechanical properties of PVA composites. As shown in Figure 2, CTS was uniformly dispersed in the PVA matrix in all samples. Some blurred-phase interfaces between PVA and CTS indicated that the compatibility of the two components improved during the S^3M process. Clearly, the cell structure of CTS was destroyed and the hydrogen bonds between cellulose, hemicellulose, and lignin were dissociated, resulting in better accessibility, dispersion, and compatibility in the PVA matrix.[40]

The molecular interaction was first analyzed by FTIR (Figure 3a), and the detailed peak characterization is summarized in the Supporting Information. Most importantly, both CTS and PVA presented broad OH stretching vibrations at 3395 and 3340 cm^{-1}, respectively.[41] The ratio of A_{-H-}/A_{-CH_2} was taken as an indicator to evaluate the intensity of hydrogen bonding, as shown in Table 1. The ratio in CTS is far lower than that in PVA,

Table 1. FTIR Analysis of PVA/CTS Composites

	transmittance (%)		
sample	A_{-CH_2}(2940.84 cm^{-1})	A_{-H-}(3340 cm^{-1})	A_{-H-}/A_{-CH_2}
PVA	94.4	87.9	0.931
CTS	40.6	30.4	0.749
PVA-CTS-10	93.6	87.4	0.934
PVA-CTS-20	95.1	90.3	0.950
PVA-CTS-30	94.4	88.4	0.936
PVA-CTS-40	94.6	89.5	0.946

demonstrating the low intramolecular hydrogen bonding effect. Interestingly, after the S^3M treatment, the ratio in the PVA/CTS composites slightly increased compared with that in pure PVA. Under the shearing and peeling action of solid-state mechanochemistry, the inter-embedded hydroxyl groups in CTS were gradually exposed and interacted with a large number of free hydroxyl groups in PVA, which increased the intensity of the hydroxyl peaks.

https://doi.org/10.1021/acsomega.2c05810
ACS Omega 2022, 7, 42515−42523

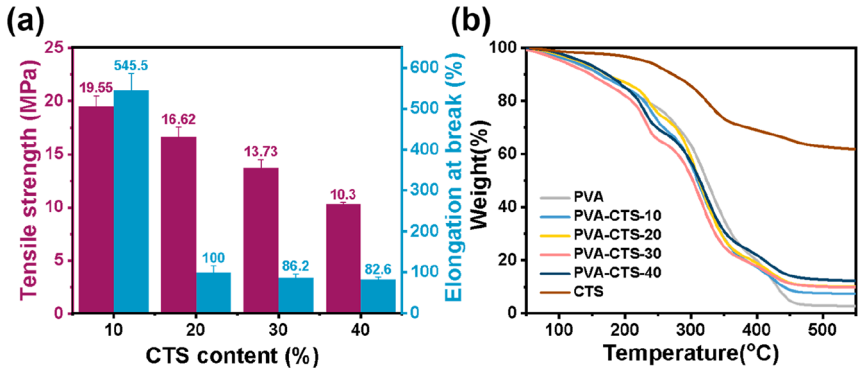

Figure 4. (a) Effect of the content of CTS on the mechanical performance of the PVA/CTS composites. (b) TGA curves of various composite sheets.

As foreign fillers, biomass particles can form a heterogeneous nucleation site in the matrix, impacting the crystallinity of the composite sheets.[42] As shown in Figure 3b, PVA and the composites showed a strong and sharp peak at $2\theta = 19.7°$ and a shoulder peak at $2\theta = 22.8°$ ascribable to the (101) and (200) crystal planes of PVA,[43] respectively. Meanwhile, the peak at $2\theta = 20.8°$ corresponded to cellulose in CTS.[44] With the increasing CTS content, the diffraction peaks of cellulose ($2\theta = 20.8°$) gradually became pronounced. The DSC curves of the PVA composites with various CTS contents are shown in Figure 3c. The endothermic peak appeared at around 170 °C, corresponding to the melting point of PVA. With the incorporation of CTS, the melting point of the composites first increased from 169.9 to 177.9 °C (PVA-CTS-20) and then decreased to 168.6 °C. The crystallinity of samples displayed the same trend as shown in Figure 3d. The high loading of the biomass particles causes steric hindrance, which impedes the fold-back of molecular chains to form thinner lamellae and accordingly decreases both the melting temperature and the crystallinity.

Mechanical and Thermal Stability of the PVA/CTS Composites. The tensile test was conducted to determine the effect of filler loading on the mechanical properties of the composites (Figure 4a). With the addition of CTS, the tensile strength of the PVA/CTS composites decreased from 19.55 (10 wt %) to 10.3 MPa (40 wt %) while the elongation at break reduced from 545.5% to 82.6%, respectively. It is notable that a compatibilizer was not incorporated in the matrix considering the possible environmental toxicity. Although the intramolecular interaction between PVA matrix and CTS cannot ensure reliable compatibility, the active functional group exposed by S^3M processing indeed promoted the dispersion of fillers and prevented an unacceptable deterioration in mechanical performance. The mechanical performance and micrograph of the PVA/biomass composites without S^3M are shown in the Supporting Information (Figure S1).

Thermal stability is essential for the practical application of the composite material. As shown in Figure 4b, the thermogravimetric behavior of composites has three stages. The first stage observed at around 100−250 °C was ascribed to the evaporation of plasticizers (deionized water and glycerin), with a weight loss of 30%. The second stage of the thermal degradation of the composites occurred from 270 to 380 °C due to acetate group elimination in PVA and the degradation of the polymeric network in hemicellulose and cellulose. The third stage of composite degradation occurred between 400 to 500 °C, which was attributed to lignin degradation and the breakdown of the polymer backbone in PVA. The thermal stability was quantitatively analyzed by the heat-resistance index (T_{HRI}), and the results are summarized in Table 2. The composites exhibited slightly decreased T_{HRI} compared to both PVA and CTS. He[40] demonstrated that S^3M can effectively decrease the crystallinity of PVA and simultaneously result in more crystal lattice distortions and defects, offsetting the benefits of high-thermal-stability CTS.

Table 2. Characteristic Thermal Data of PVA/CTS Composites

	weight loss temperature (°C)			
sample	5%	30%	50%	T_{HRI}[a] (°C)
PVA	117.2	280.3	324.3	105.4
CTS	231.3	385.5	>700	158.7
PVA-CTS-10	119.3	258.4	310.2	99.4
PVA-CTS-20	130.2	276.5	312.7	106.81
PVA-CTS-30	104.5	235.6	302.9	89.8
PVA-CTS-40	134.7	248.0	313.5	99.3

[a] $T_{HRI} = 0.49 \times [T_5 + 0.6 \times (T_{30} - T_5)]$. T_5 and T_{30} represent the decomposition temperatures corresponding to 5 and 30 wt % weight loss, respectively.

Environmental Friendliness of the PVA/CTS Composites. In general, the weight loss in the soil burial test is a typical indicator of degradation. However, as shown in the Supporting Information (Figure S2), the border between specimens and the soil became indistinct within three days, and all samples were merged with the soil within eight days under the earth. This significant deformation indicated an undeniable interaction between the soil environment and the PVA-based composites, which may come from two aspects. On one hand, PVA is a typical water-soluble polymer, making it likely to be dissolved by the water in the soil; on the other hand, PVA is also a biodegradable polymer that can be decomposed by specific bacteria. For verification, the morphologies and functional groups of the PVA/CTS composites after eight days of burial were observed by SEM and FTIR, and the data are shown in the Supporting Information (Figures S3 and S4). As evidenced by the existing fiber and film, PVA was merely adhered to the soil, while the ketone group, which was supposed to exist along with the degradation reaction, was absent during the progress. Unambiguously, PVA cannot be directly degraded in the environment. Although PVA-based composites dissolved in soil, it was necessary to evacuate its influenced on the soil; this influence was analyzed using wheat and earthworm growth tests. As recorded in Figure 5, the average growth height of wheat eventually reached ~15 cm, indicating that neither PVA nor CTS content had an obvious effect on the soil.

https://doi.org/10.1021/acsomega.2c05810
ACS Omega 2022, 7, 42515−42523

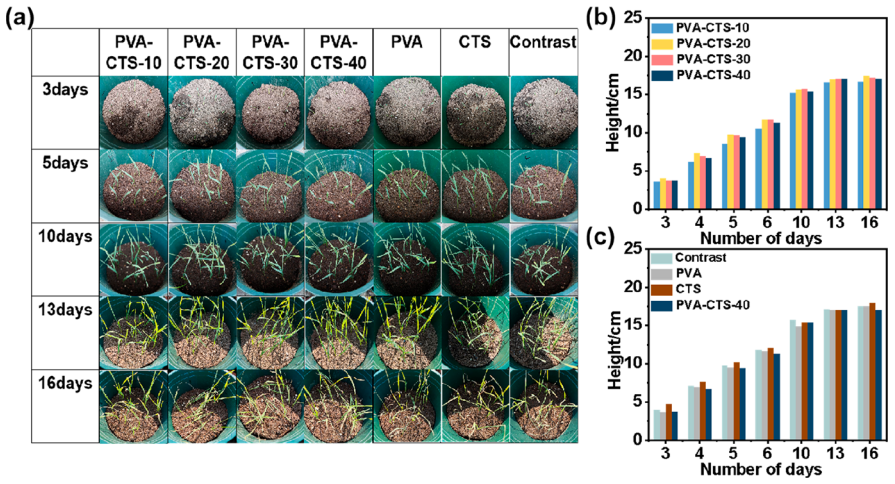

Figure 5. (a) Pictures of the growth status of the wheat. (b and c) Average height histograms of the wheat in pots with different kinds of sample buried.

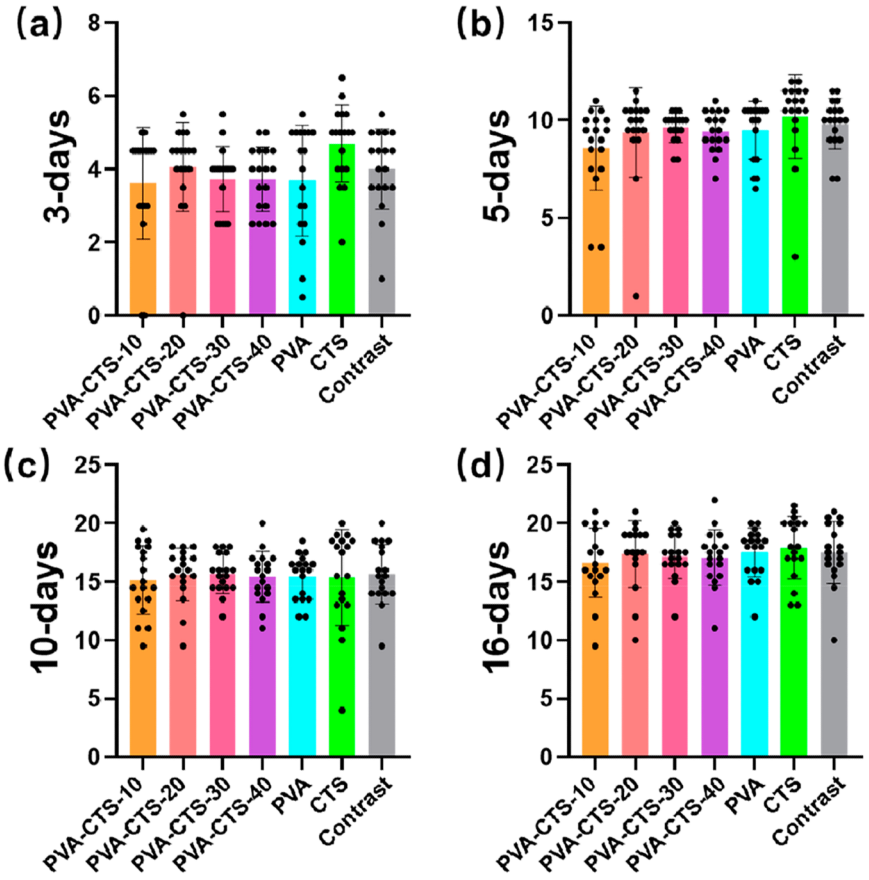

Figure 6. Mean histogram parameters of the height of the wheat seeded on pots with different kinds of samples after (a) 3, (b) 5, (c) 10, and (d) 16 days (n = 18).

Table 3. *P* Values of the above Samples on the 3rd, 5th, 10th, and 16th Days[a]

time	A-G	B-G	C-G	D-G	E-G	F-G
3 days	0.9950	>1	0.9996	0.9996	0.9992	0.8098
5 days	0.6629	0.9996	>1	0.9999	>1	>1
10 days	>1	>1	>1	>1	>1	>1
16 days	0.9989	>1	>1	>1	>1	>1

[a]A = PVA-CTS-10, B = PVA-CTS-20, C = PVA-CTS-30, D = PVA-CTS-40, E = PVA, F = CTS, and G = Contrast.

For a quantitative analysis, the difference between the experimental and control groups in terms of wheat height was analyzed by a one-way analysis of variance (ANOVA) test with Tukey's multiple comparisons test in which $P < 0.05$ was

https://doi.org/10.1021/acsomega.2c05810
ACS Omega 2022, 7, 42515−42523

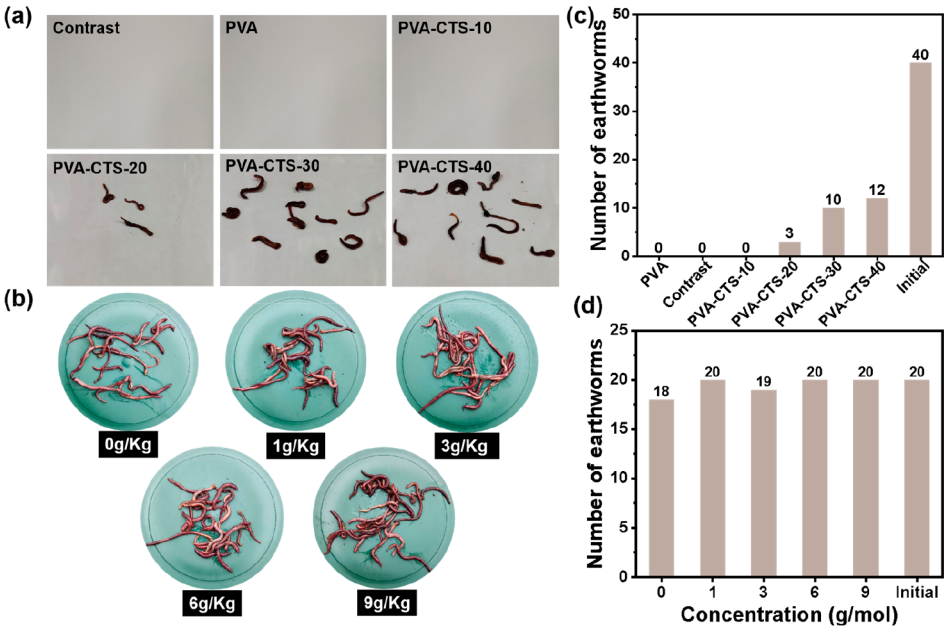

Figure 7. Digital photos of the surviving earthworms as a function of content of (a) biomass filler and (b) PVA solution and (c and d) the corresponding statistical data.

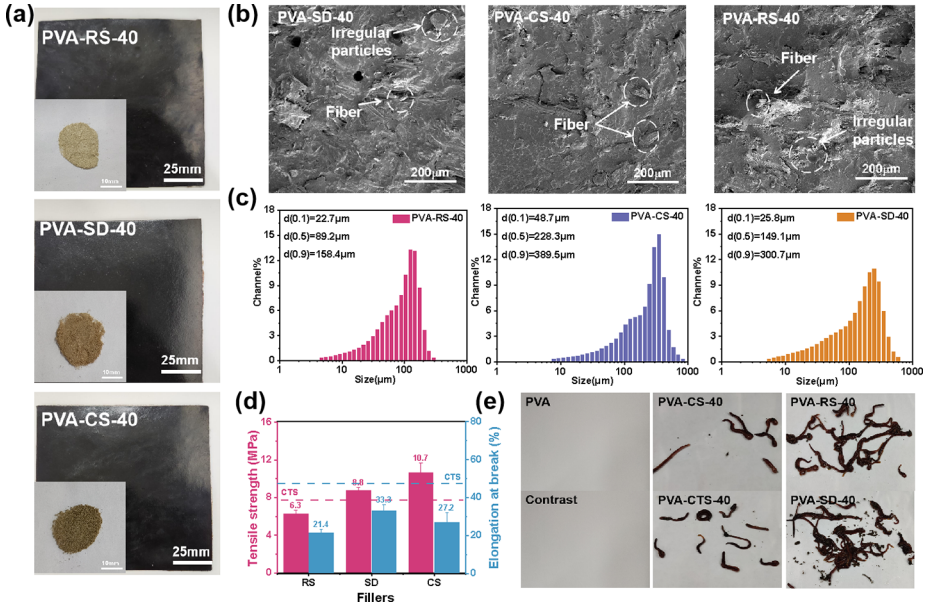

Figure 8. Morphology and performance of PVA/RS, PVA/CS, and PVA/SD composites. (a) Digital and (b) SEM photos of the various PVA/biomass composites and (c) the corresponding particle distribution. (d) Mechanical and (e) environmental performance of the various PVA/biomass composites.

considered significant. All statistical analyses were performed by GraphPad Prism software (ver. 8.02). The mean histogram parameters of the height of the wheat after 3, 5, 10, and 16 days are displayed in Figure 6 and Table 3. Since all the P values of samples were higher than 0.05, it can be concluded that no statistical difference was found between the experimental and control groups ($P > 0.05$). Therefore, the incorporation of PVA/CTS composites did not impose adverse effects on the growth of the wheat.

Earthworms play a significant role in soil formation and nutrient cycling, which are regarded as biological indicators of the soil ecosystem. Therefore, earthworms were used to evaluate the effect of biocomposites on soil biota in this study. The growth status of the earthworms is shown in Figure 7a and b. According to Figure 7c, there were no survivors in PVA and Pot-CTS-10, but the number of surviving earthworms increased with the content of the biomass fillers. Earthworms feed on organic matter in the soil, and PVA, as a polymer, cannot be digested and absorbed by earthworms. Therefore, the decreased number of earthworms should be ascribed to lack of nutrients. More evidence is presented in Figure 7d, which shows there were no evident changes in the number of earthworms after two weeks; that is, almost all the earthworms survived equally. It can be concluded that although PVA had no obvious perceptible effect on the earthworms, it cannot provide the necessary nutrients for earthworms. Consequently, the PVA/biomass composite

https://doi.org/10.1021/acsomega.2c05810
ACS Omega 2022, 7, 42515−42523

displayed an environmentally friendly nature and great potential for practical application.

Universality of the PVA/Biomass Composites. Due to the different compositions of cellulose in various biomass waste, which may cause variations in performance, another three kinds of biomass waste were used in this study, i.e., RS, SD, CS. The as-prepared powders and composites were named PVA-RS-40, PVA-SD-40, and PVA-CS-40, respectively. As displayed in Figure 8a and b, all biomass waste was evenly distributed in the PVA matrix via the pulverization and mixing effect of the S^3M technology. Figure 8c shows the volume-based particle size distribution of the composite powder. The average particle size of all composite powder was less than 300 μm. In general, a smaller particle size leads to a smaller domain size and thus endows composites with better compatibility, which determines the interaction and dispersion of fillers in the PVA matrix. The tensile strength of the composites was 13.5, 12, and 8.5 MPa for PVA-RS-40, PVA-SD-40, and PVA-CS-40, respectively, while the elongation at break was 21.4%, 33.3%, and 27.2% (Figure 8d). Obviously, the type of biomass waste had little impact on the mechanical performance of the composites. The environmental friendliness also exhibited the same trend, as shown in Figure 8e, which is rationalized by the fact that the main components of biomass waste are cellulose, hemicellulose, and lignin. Unambiguously, the water-soluble PVA/biomass composites exhibited universality and adaptability to most biomass waste and thus the potential for practical application.

CONCLUSION

In this work, the concept of ecofriendly water-soluble composites was demonstrated by PVA/biomass composites. Although the mechanical performance and thermal stability of the PVA-based composites declined with the incorporation of the biomass waste, the as-prepared PVA/CTS composites exhibited a maximum tensile strength of 10.3 MPa and a degradation temperature of ~250 °C, which met the demand for practical applications. Most importantly, it was confirmed by SEM and FTIR that the biocomposites could quickly dissolve in soil before PVA was biodegraded by microorganisms. The dissolved PVA imposes no adverse effects on animals or plants, which ensures its environmental friendliness. This work has offered a new method to reduce the amount of discarded plant waste and fabricate green alternatives of conventional plastics to contribute to resource utilization and environmental protection.

ASSOCIATED CONTENT

Supporting Information

The Supporting Information is available free of charge at https://pubs.acs.org/doi/10.1021/acsomega.2c05810.

Detailed FTIR peak characterization, mechanical performance of the PVA/biomass composites sheet without S^3 M processing, photos of PVA/biomass composites in the soil burial test, SEM image of the PVA/CTS composite buried for eight days, and FTIR curves of the PVA/CTS composite buried for eight days (PDF)

AUTHOR INFORMATION

Corresponding Author

Yijun Li − *State Key Laboratory of Polymer Materials Engineering, Polymer Research Institute of Sichuan University, Sichuan University, Chengdu, Sichuan 610065, China;* orcid.org/0000-0002-6788-0730; Email: ruddph@gmail.com

Authors

Guoliang Tian − *State Key Laboratory of Polymer Materials Engineering, Polymer Research Institute of Sichuan University, Sichuan University, Chengdu, Sichuan 610065, China*

Li Li − *State Key Laboratory of Polymer Materials Engineering, Polymer Research Institute of Sichuan University, Sichuan University, Chengdu, Sichuan 610065, China;* orcid.org/0000-0002-3576-4372

Qi Wang − *State Key Laboratory of Polymer Materials Engineering, Polymer Research Institute of Sichuan University, Sichuan University, Chengdu, Sichuan 610065, China*

Complete contact information is available at: https://pubs.acs.org/10.1021/acsomega.2c05810

Notes

The authors declare no competing financial interest.

ACKNOWLEDGMENTS

This work is kindly supported by the National Natural Science Foundation of China (U21A2091, 51720105012, and 51873073).

REFERENCES

(1) Wan, K.; Chen, H.; Zheng, F.; Pan, Y.; Zhang, Y.; Long, D. Tunable Production of Jet-Fuel Range Alkanes and Aromatics by Catalytic Pyrolysis of LDPE over Biomass-Derived Activated Carbons. *Ind. Eng. Chem. Res.* **2020**, *59* (39), 17451−17461.

(2) Zhang, F.; Zhao, Y.; Wang, D.; Yan, M.; Zhang, J.; Zhang, P.; Ding, T.; Chen, L.; Chen, C. Current technologies for plastic waste treatment: A review. *Journal of Cleaner Production* **2021**, *282*, No. 124523.

(3) Kabir, E.; Kaur, R.; Lee, J.; Kim, K.-H.; Kwon, E. E. Prospects of biopolymer technology as an alternative option for non-degradable plastics and sustainable management of plastic wastes. *Journal of Cleaner Production* **2020**, *258*, No. 120536.

(4) Han, Y.; Shi, J.; Mao, L.; Wang, Z.; Zhang, L. Improvement of Compatibility and Mechanical Performances of PLA/PBAT Composites with Epoxidized Soybean Oil as Compatibilizer. *Ind. Eng. Chem. Res.* **2020**, *59* (50), 21779−21790.

(5) Sanchez-Hernandez, J. C.; Capowiez, Y.; Ro, K. S. Potential Use of Earthworms to Enhance Decaying of Biodegradable Plastics. *ACS Sustainable Chem. Eng.* **2020**, *8* (11), 4292−4316.

(6) Gao, D.; Lv, J.; Lee, P. S. Natural Polymer in Soft Electronics: Opportunities, Challenges, and Future Prospects. *Adv. Mater.* **2022**, *34* (25), No. 2105020.

(7) Cao, H.; Wang, X. Carbon dioxide copolymers: Emerging sustainable materials for versatile applications. *SusMat* **2021**, *1* (1), 88−104.

(8) Wang, G. X.; Huang, D.; Ji, J. H.; Volker, C.; Wurm, F. R. Seawater-Degradable Polymers-Fighting the Marine Plastic Pollution. *Adv. Sci. (Weinh)* **2021**, *8* (1), No. 2001121.

(9) Briassoulis, D.; Tserotas, P.; Athanasoulia, I.-G. Alternative optimization routes for improving the performance of poly(3-hydroxybutyrate) (PHB) based plastics. *Journal of Cleaner Production* **2021**, *318*, No. 128555.

(10) Abdal-hay, A.; Raveendran, N. T.; Fournier, B.; Ivanovski, S. Fabrication of biocompatible and bioabsorbable polycaprolactone/magnesium hydroxide 3D printed scaffolds: Degradation and in vitro osteoblasts interactions. *Composites Part B: Engineering* **2020**, *197*, No. 108158.

(11) Deng, S.; Ma, J.; Guo, Y.; Chen, F.; Fu, Q. One-step modification and nanofibrillation of microfibrillated cellulose for simultaneously reinforcing and toughening of poly(ε-caprolactone). *Compos. Sci. Technol.* **2018**, *157*, 168−177.

(12) Wasti, S.; Triggs, E.; Farag, R.; Auad, M.; Adhikari, S.; Bajwa, D.; Li, M.; Ragauskas, A. J. Influence of plasticizers on thermal and mechanical properties of biocomposite filaments made from lignin and polylactic acid for 3D printing. *Composites Part B: Engineering* **2021**, *205*, No. 108483.
(13) Liu, S.; Qin, S.; He, M.; Zhou, D.; Qin, Q.; Wang, H. Current applications of poly(lactic acid) composites in tissue engineering and drug delivery. *Composites Part B: Engineering* **2020**, *199*, No. 108238.
(14) Yeo, J. C. C.; Muiruri, J. K.; Tan, B. H.; Thitsartarn, W.; Kong, J.; Zhang, X.; Li, Z.; He, C. Biodegradable PHB-Rubber Copolymer Toughened PLA Green Composites with Ultrahigh Extensibility. *ACS Sustainable Chem. Eng.* **2018**, *6* (11), 15517−15527.
(15) Bi, S.; Pan, H.; Barinelli, V.; Eriksen, B.; Ruiz, S.; Sobkowicz, M. J. Biodegradable polyester coated mulch paper for controlled release of fertilizer. *Journal of Cleaner Production* **2021**, *294*, No. 126348.
(16) Wu, W.; Wu, C.; Peng, H.; Sun, Q.; Zhou, L.; Zhuang, J.; Cao, X.; Roy, V. A. L.; Li, R. K. Y. Effect of nitrogen-doped graphene on morphology and properties of immiscible poly(butylene succinate)/polylactide blends. *Composites Part B: Engineering* **2017**, *113*, 300−307.
(17) Zhou, S.-J.; Wang, H.-M.; Xiong, S.-J.; Sun, J.-M.; Wang, Y.-Y.; Yu, S.; Sun, Z.; Wen, J.-L.; Yuan, T.-Q. Technical Lignin Valorization in Biodegradable Polyester-Based Plastics (BPPs). *ACS Sustainable Chem. Eng.* **2021**, *9* (36), 12017−12042.
(18) Moharir, R. V.; Kumar, S. Challenges associated with plastic waste disposal and allied microbial routes for its effective degradation: A comprehensive review. *Journal of Cleaner Production* **2019**, *208*, 65−76.
(19) Oyeoka, H. C.; Ewulonu, C. M.; Nwuzor, I. C.; Obele, C. M.; Nwabanne, J. T. Packaging and degradability properties of polyvinyl alcohol/gelatin nanocomposite films filled water hyacinth cellulose nanocrystals. *Journal of Bioresources and Bioproducts* **2021**, *6* (2), 168−185.
(20) Qin, M.; Chen, C.; Song, B.; Shen, M.; Cao, W.; Yang, H.; Zeng, G.; Gong, J. A review of biodegradable plastics to biodegradable microplastics: Another ecological threat to soil environments? *Journal of Cleaner Production* **2021**, *312*, No. 127816.
(21) Ding, Q.; Xu, X.; Yue, Y.; Mei, C.; Huang, C.; Jiang, S.; Wu, Q.; Han, J. Nanocellulose-Mediated Electroconductive Self-Healing Hydrogels with High Strength, Plasticity, Viscoelasticity, Stretchability, and Biocompatibility toward Multifunctional Applications. *ACS Appl. Mater. Interfaces* **2018**, *10* (33), 27987−28002.
(22) Liu, Y.; Liu, S.; Liu, Z.; Lei, Y.; Jiang, S.; Zhang, K.; Yan, W.; Qin, J.; He, M.; Qin, S.; et al. Enhanced mechanical and biodegradable properties of PBAT/lignin composites via silane grafting and reactive extrusion. *Composites Part B: Engineering* **2021**, *220*, No. 108980.
(23) Sid, S.; Mor, R. S.; Kishore, A.; Sharanagat, V. S. Bio-sourced polymers as alternatives to conventional food packaging materials: A review. *Trends in Food Science & Technology* **2021**, *115*, 87−104.
(24) Xiong, F.; Wu, Y.; Li, G.; Han, Y.; Chu, F. Transparent Nanocomposite Films of Lignin Nanospheres and Poly(vinyl alcohol) for UV-Absorbing. *Ind. Eng. Chem. Res.* **2018**, *57* (4), 1207−1212.
(25) Haque, A. N. M. A.; Naebe, M. Flexible water-resistant semi-transparent cotton gin trash/poly (vinyl alcohol) bio-plastic for packaging application: Effect of plasticisers on physicochemical properties. *Journal of Cleaner Production* **2021**, *303*, No. 126983.
(26) Aloui, H.; Khwaldia, K.; Hamdi, M.; Fortunati, E.; Kenny, J. M.; Buonocore, G. G.; Lavorgna, M. Synergistic Effect of Halloysite and Cellulose Nanocrystals on the Functional Properties of PVA Based Nanocomposites. *ACS Sustainable Chem. Eng.* **2016**, *4* (3), 794−800.
(27) Han, J.; Wang, S.; Zhu, S.; Huang, C.; Yue, Y.; Mei, C.; Xu, X.; Xia, C. Electrospun Core-Shell Nanofibrous Membranes with Nanocellulose-Stabilized Carbon Nanotubes for Use as High-Performance Flexible Supercapacitor Electrodes with Enhanced Water Resistance, Thermal Stability, and Mechanical Toughness. *ACS Appl. Mater. Interfaces* **2019**, *11* (47), 44624−44635.
(28) Wu, F.; Misra, M.; Mohanty, A. K. Sustainable green composites from biodegradable plastics blend and natural fibre with balanced performance: Synergy of nano-structured blend and reactive extrusion. *Compos. Sci. Technol.* **2020**, *200*, No. 108369.
(29) Zhou, B.; Wang, L.; Ma, G.; Zhao, X.; Zhao, X. Preparation and properties of bio-geopolymer composites with waste cotton stalk materials. *Journal of Cleaner Production* **2020**, *245*, No. 118842.
(30) Hu, D.; Zeng, M.; Sun, Y.; Yuan, J.; Wei, Y. Cellulose-based hydrogels regulated by supramolecular chemistry. *SusMat* **2021**, *1* (2), 266−284.
(31) Han, J.; Ding, Q.; Mei, C.; Wu, Q.; Yue, Y.; Xu, X. An intrinsically self-healing and biocompatible electroconductive hydrogel based on nanostructured nanocellulose-polyaniline complexes embedded in a viscoelastic polymer network towards flexible conductors and electrodes. *Electrochim. Acta* **2019**, *318*, 660−672.
(32) Han, J.; Wang, H.; Yue, Y.; Mei, C.; Chen, J.; Huang, C.; Wu, Q.; Xu, X. A self-healable and highly flexible supercapacitor integrated by dynamically cross-linked electro-conductive hydrogels based on nanocellulose-templated carbon nanotubes embedded in a viscoelastic polymer network. *Carbon* **2019**, *149*, 1−18.
(33) Haque, A. N. M. A.; Remadevi, R.; Wang, X.; Naebe, M. Biodegradable cotton gin trash/poly(vinyl alcohol) composite plastic: Effect of particle size on physicochemical properties. *Powder Technol.* **2020**, *375*, 1−10.
(34) Balavairavan, B.; Saravanakumar, S. S. Characterization of Ecofriendly Poly (Vinyl Alcohol) and Green Banana Peel Filler (GBPF) Reinforced Bio-Films. *Journal of Polymers and the Environment* **2021**, *29* (9), 2756−2771.
(35) Chen, G.; Chen, N.; Li, L.; Wang, Q.; Duan, W. Ionic Liquid Modified Poly(vinyl alcohol) with Improved Thermal Processability and Excellent Electrical Conductivity. *Ind. Eng. Chem. Res.* **2018**, *57* (15), 5472−5481.
(36) Yang, S.; Bai, S.; Wang, Q. Sustainable packaging biocomposites from polylactic acid and wheat straw: Enhanced physical performance by solid state shear milling process. *Compos. Sci. Technol.* **2018**, *158*, 34−42.
(37) Liu, X.; Li, Y.; Zeng, L.; Li, X.; Chen, N.; Bai, S.; He, H.; Wang, Q.; Zhang, C. A Review on Mechanochemistry: Approaching Advanced Energy Materials with Greener Force. *Adv. Mater.* **2022**, No. 2108327.
(38) Wu, Q.; Chen, N.; Wang, Q. Crystallization behavior of melt-spun poly(vinyl alcohol) fibers during drawing process. *Journal of Polymer Research* **2010**, *17* (6), 903−909.
(39) Fujii, K.; Imoto, S.; Ukida, J.; Matsumoto, M. On the stereoregulation in polymerization of vinyl formate. *Journal of Polymer Science Part B: Polymer Letters* **1963**, *1* (9), 497−499.
(40) He, P.; Bai, S.; Wang, Q. Structure and performance of Poly(vinyl alcohol)/wood powder composite prepared by thermal processing and solid state shear milling technology. *Composites Part B: Engineering* **2016**, *99*, 373−380.
(41) Haque, A. N. M. A.; Remadevi, R.; Wang, X.; Naebe, M. Sorption properties of fabricated film from cotton gin trash. *Materials Today: Proceedings* **2020**, *31*, S221−S226.
(42) Liu, B.; Li, Y.; Wang, Q.; Bai, S. Green fabrication of leather solid waste/thermoplastic polyurethanes composite: Physically de-bundling effect of solid-state shear milling on collagen bundles. *Compos. Sci. Technol.* **2019**, *181*, 107674.
(43) Deng, F.; Guan, Y.; Shi, Z.; Wang, F.; Che, X.; Liu, Y.; Wang, Y. The effect of dopamine modified titanium dioxide nanoparticles on the performance of Poly (vinyl alcohol)/titanium dioxide composites. *Compos. Sci. Technol.* **2017**, *150*, 120−127.
(44) Yao, W.; Weng, Y.; Catchmark, J. M. Improved cellulose X-ray diffraction analysis using Fourier series modeling. *Cellulose* **2020**, *27* (10), 5563−5579.

https://doi.org/10.1021/acsomega.2c05810
ACS Omega 2022, 7, 42515−42523